Chapter 6
Pulmonary Metastasis

Anastasia Malek

Abstract Metastases are the leading cause of death among cancer patients; furthermore, the lungs are the most common site of tumor dissemination. Better understanding of the molecular mechanisms underlying pulmonary colonization by circulating cancer cells could improve the quality of life and survival rate for patients. It definitely requires well-designed experimental systems.

This chapter presents a short review of the main biological aspects of pulmonary metastases and describes approaches to model metastatic processes in the lung *in vitro*, *ex vivo*, and *in vivo* with emphasis on experimental settings and applicability. In addition, the basic techniques for evaluation and analysis of experimental lung metastases are discussed. Finally, a qPCR-based method of detection and quantification of metastatic tumor burden in human xenograft models of pulmonary metastases is presented. Overall, the chapter content provides a methodological background for the experimental study of secondary lung cancer.

Abbreviations

CUP	Carcinoma of unknown primary
CT	Computed tomography
PET	Positron emission tomography
RFA	Radiofrequency ablation
SBRT	Stereotactic body radiotherapy
VP	Vascular permeability
V_C	Capillary volume
S_A	Alveolar surface area
GFP	Green fluorescent protein
NIR	Near infra-red
CTC	Circulating cancer cells
Luc	Luciferase
IHC	Immunihistochemistry
qPCR	Quantitative polymerase chain reaction

A. Malek (✉)
Department of Oncoendocrinology, Petrov Institute of Oncology, Sankt-Petersburg, Russia
e-mail: anastasia@malek.com

A. Malek (ed.), *Experimental Metastasis: Modeling and Analysis,*
DOI 10.1007/978-94-007-7835-1_6,

6.1 Introduction–Clinical Relevance of Pulmonary Metastasis

Approximately one out of 1,000 chest radiographs show the incidental finding of a pulmonary lesion caused by a tumor [1]. Unfortunately, only a small percentage (2-5 %) of lung tumors are of benign origin, e.g., lipomas, fibromas, hamartomas, and chondromas; the majority are malignant neoplasms, most commonly primary lung cancer, followed by metastases of extrapulmonary primary carcinomas. The lungs are among the most prominent target organs for metastatic disease. Most frequently, lung metastases originate from cancers of the breast, colon, head and neck, stomach, pancreas, kidney, bladder, the male and female genitourinary tract, and sarcomas. Lung metastases occur in approximately 30 % of patients dying of cancer and can reduce the quality of life for many patients living with advanced cancer. Pulmonary metastatic disease can be defined as a separate nosologic category since this condition requires specific diagnostic [2] and treatment approaches [3, 4].

Symptoms considered as clinical indications of secondary lung tumors are chest pain, dyspnea, cough, or hemoptysis. However, either an advanced metastatic process or specific localization of certain metastases may manifest by such symptoms, while the initial stages of pulmonary metastatic disease are usually silent clinically. A scenario that is not infrequently encountered is an incidental finding of secondary lung cancer of unknown origin, a so-called carcinoma of unknown primary (CUP), when patients are undergoing screening chest radiography, computed tomography (CT) scanning, or positron emission tomography (PET)/CT scanning. Radiographically, secondary lung tumors usually appear as discrete nodules (single or multiple), interstitial infiltrates, or endobronchial lesions with or without distal atelectasis or postobstructive pneumonitis. They often have a characteristic round appearance on chest radiographs.

Management of secondary lung cancer presents a challenge for the oncologist. There are a number of curative approaches including surgery, systemic chemotherapy or local chemo-perfusion, radiation, and immunotherapy; however, the most appropriate treatment plan depends on the number, location, and size of the metastases, the pathologic diagnosis of the primary tumor if known, and patient status. Several studies demonstrated a survival benefit from complete resection of all pulmonary metastases originating from breast [5] or colorectal cancers [6]. In some patients pulmonary metastasectomy may even be the only curative treatment option. Generally accepted rules for intended curative pulmonary metastasectomy are control of the primary tumor, technically completely resectable metastases, the exclusion of extrapulmonary metastases (except for potentially completely resectable hepatic metastases) and functional operability. The most important prognostic factors are complete resection, the exact entity of the tumor, and disease-free interval [3, 7]. The chemotherapeutic approach for lung metastases treatment is usually defined by the pathologic diagnosis of the primary tumor. However, many patients develop recurrent disease in the thorax despite the use of systemic chemotherapy, the dosage of which is limited by systemic toxicity. Similar to the basic principles of isolated limb and liver perfusion, isolated lung perfusion is an attractive and

promising surgical technique for the delivery of high-dose chemotherapy with minimal systemic toxicity [4]. Advanced techniques of localized radiotherapy, such as radiofrequency ablation (RFA) or stereotactic body radiotherapy (SBRT), may be considered as a method of choice or adjunctive therapy [8].

The appearance lung metastases defines the late (or disseminated) stage of cancer of any origin. Despite advanced curative approaches and individualized multimodal strategy applied for each patient, the prognosis of metastatic lung cancer is generally poor with only a slight difference among primary tumor types. The National Cancer Institute's (USA) statistics (2003–2009) for advanced cancer 5-years survival rate [9] provides the following numbers: breast cancer, 24.3 %; colorectal cancer, 12.5 %; bladder cancer, 5.4 %; pancreatic cancer, 2 %, and stomach cancer, 3.9 %. Considering the fact that the lungs are the primary site of distant metastases of these cancer types, the overall survival rate associated with pulmonary metastatic disease is currently disappointing. Among patients with cancer of unknown primary (CAP), pulmonary metastatic disease represents the most common cause of death with a median survival of 3 months [10].

6.2 General Consideration of Pulmonary Metastasis

Several factors could be considered to play a major role in pathogenesis of the lung metastasis: particularity of pulmonary blood circulation, adhesive properties and permeability of pulmonary endothelium mediating interaction with and extravasation of circulating tumor cells (CTC), local (pulmonary) specificity of host immune system.

6.2.1 Structure of the Vascular Bed

Detached tumor cells entre into the bloodstream through the venous drainage, after passing the right hart and arteries pulmonary, they reach the lungs and are retained in pulmonary capillaries. Thus, lung parenchyma is the most common site of bloodstream-mediated metastasis due to filtering capacity of pulmonary capillary net. Since blood oxygenation is a main physiological function of the lung, its vascular (arterial and venous) tree has an extremely branched structure. As it was estimated in early studies by integrated morphometric analysis, the human pulmonary arterial tree is comprised of 17 branch orders, from the main pulmonary artery (order 17) with a diameter of ~ 30 mm to more than 72 million order 1 arteries which range in diameter from 10–15 μm [11]. In context of this chapter, it is important to consider difference between human and rat lung. In contrast to the 15–17 orders of pulmonary artery branches in human lung, in smaller mammals such as rat, the pulmonary arterial tree is comprised of only 11–12 orders. As would be expected, the number of distal order 1 branches decreases with body mass. For example, in dog and rat lung the number of order 1 branches is estimated to be ~1 and 3 log orders less,

respectively, than that in human lung. However, the diameter of these distal precapillary order 1 branches is similar from human to rat lung [12].

One more specific feature of pulmonary vasculature is a density and spatial heterogeneity of the capillary net. Capillary networks adjacent to bronchovascular bundles and in the subpleural network are comprised of long tubular segments, similar in organization to those capillary networks seen in many systemic vascular beds. In contrast, shorter capillary segments are present in the much more dense capillary networks which occupy alveolar septal walls [13, 14]. This structural feature may be reflected by specific pattern of lung metastases distribution. There is also difference in lung capillary density among species. Thus, overall capillary loading or capillary density in the septal compartment in lung can be estimated by the ratio of total capillary volume (V_C) to total alveolar surface area (S_A). Based on data provided by Gehr and colleagues in their comprehensive assessment of scaling in the respiratory system, the V_C/S_A ratio increases from 1.18 in mouse lung to 1.24, 1.43, and 1.49 in rat, dog and human lung, respectively [15]. These data suggest that the alveolar capillary network is somewhat denser in larger mammals (human) that may result to higher predisposition to metastases development in comparison with laboratory animals.

In additional to anatomical/structural features of vascular bed, vascular permeability (VP) presents an essential and highly regulated factor implemented in metastatic process in the lung. Evidence suggests that cancer cells need to weaken the interendothelial junctions in order to cross the endothelial barrier. Several tumor-derived vasoactive compounds have been pointed out to drive increase in vascular permeability: VEGF, Angptl4, CCL2, SDF-1, etc [16, 17]. Src kinase of pulmonary endothelial cells was evaluated as a point of convergence for many of these regulatory pathways. An essential role of Src in extravasation of tumor cells from lung capillaries was demonstrated when direct intravenous injection of cancer cells resulted in a more than 2-fold reduction in lung tumor burden in src-null mice compared to control animals [18]. Results of this study, in both experimental metastasis and spontaneous metastasis models, revealed implication of Src-mediated VP in tumor metastasis to the lung.

6.2.2 Adhesive Properties and Cell-Cell Interaction

Besides vascular anatomy, proper characteristics of CTC can mediate pattern and intensity of metastatic process. As long ago as 1889, Stephen Paget proposed that metastasis depends on cross-talk between selected cancer cells (the ‘seeds’) and specific organ microenvironments (the ‘soil’) [19]. This hypothesis, so called “seed and soil”, still holds forth today [20]. As it is postulated now, the potential of a tumor cell to metastasize depends on its interactions with the homeostatic factors that promote tumor-cell growth, survival, angiogenesis, invasion and metastasis. In addition, some surface molecules of metastatic cells have affinity to capillary of certain tissue that defines preferential, not random, colonization of secondary organs.

Evidence for this phenomenon has been demonstrated in early studies by the preferential adhesion of metastatic tumor cells to vascular endothelial cells isolated from metastasized organs. For example, lung-metastatic tumor cells adhere preferentially to monolayers of lung-derived endothelial cells, whereas brain-metastatic glioma cells, liver-metastatic lymphoma cells, and ovary-metastatic teratoma cells adhere preferentially to endothelial cells isolated from brain, liver, and ovary, respectively [21, 22]. Structural and functional properties of various adhesive molecules and their implementation in the metastatic process are discussed explicitly in recent literature [23, 24].

Involvement of certain surface molecules in pulmonary metastasis is studied widely now. For instance, the chemokine receptor CXC4 was shown to be implicated in the lung specificity of breast tumor metastases, where the tissue-specific activity of its ligand CXCL12 allows chemokine-mediated signal activation [25]. Involvement of connexin-43 in colonization of the lung by circulating breast cancer cells was demonstrated in other study [26]. Mediation of lung metastasis of murine melanomas by a lung-specific endothelial cell adhesion molecule localazed on endothelia of distinct branches of lung blood vessels was demonstrated in early studies [27]. Role of integrins and selectins in lung—specific anchorage of colon cancer cells was analyzed recently by quantitative in vivo microscopy [28]. Translocation of oligosaccharides –binding lysosome associated membrane protein (LAMP1) to surface membrane and resulting over-representation of oligosaccharids (polylacNAc) specifically binding Galectin-3 was observed in melanoma cells. Since Gelectin-3 is expressed in highest amount in the lung as compared to other organs, this receptor-ligand interaction is considered to mediate lung-specific metastasis of melanomas [29].

Blood component may interact with CTC increasing their metastatic potency. For instance, CD154 expressed on and released from activated platelets induces an inflammatory response in endothelial cells and monocytes, including tissue factor production. CD154 has also been shown to activate platelets *in vitro* and promote thrombus stability *in vivo*. These CD154 effects may be mediated, at least in part, by CD40 signaling on platelets and vascular endothelial cells. Thus, Ingersoll and colleagues hypothesized that CD40 and CD154 promote lung metastases formation in experimental metastasis in mice [30]. The hypothesis was confirmed by observation that mice deficient in blood compartment CD40 had fewer lung nodules compared to wild-type mice and mice deficient in endothelial CD40. These results suggested an important contribution of the CD40/CD154 pathway to experimental lung metastasis. Furthermore, the data pointed to a selective role for peripheral blood cells in metastatic process.

6.2.3 Impact of Pulmonary Immune System

From an immunological point of view, various lymphocyte subsets have different requirements for trafficking to various organs including primary and secondary lymphoid tissues as well as non-lymphoid organs. It is possible that there are

organ-specific immune responses that might be able to eliminate a metastatic clone in one organ but not another. It has been shown that neutrophils may regulate lung metastasis development through physical interaction and anchoring of circulating tumor cells to endothelium [31]. In this study, human melanoma cells were i.v. injected into nude mice leading to the entrapment of many cancer cells. However, 24 h later, very few cancer cells remained in the lungs. In contrast, injection of human neutrophils an hour after tumor cell injection increased cancer cell retention by approximately 3-fold. Entrapped melanoma cells produced and secreted high levels of a cytokine, interleukin-8 (IL-8), attracting neutrophils and increasing tethering ß2-integrin expression by 75 to 100 %. As it was demonstrated, intercellular adhesion molecule-1 on melanoma cells and ß2-integrin on neutrophils interacted, promoting anchoring to pulmonary endothelium [31].

Moreover, the organ-specific NK cell subsets may play a critical role in organ-specific metastasis. In recent study of Ballas and colleagues, B16 murine melanoma cells readily colonized the lungs but not the liver after intravenous injection. Analysis of NK cell subsets, defined by the differential expression of a combination of CD27 and CD11b, indicated a significant difference in the distribution of NK cell subsets in the lung and liver with the mature subset being dominant in the lung and the immature subset being dominant in the liver. Several experimental approaches, including adoptive transfer, clearly indicated that the immature hepatic NK cell subset, CD27+CD11b–, was protective against liver metastasis; this subset mediated its protection by a perforin-dependent cytotoxic mechanism. In contrast, the more mature NK cell subsets were more efficient at reducing pulmonary tumor load. These data indicated that organ-specific immune responses may play a pivotal role in determining the permissiveness of a given organ for the establishment of a metastatic niche. [32]

Role of macrophages was investigated by Jordan and colleagues [33]. It was shown that activation of macrophages by natural anti-neoplastic compound (Cordyceps sinensis) reduces lung metastasis occurrence in a surgical excision model of metastatic mammary carcinoma while does not influence on primary tumor growth. This result suggested that pulmonary macrophages are also involved in control of lung colonization by cancer cells [33]

Taken together, these data reveals complex and intricate mechanism of lung—specific metastasis, suggesting an active role of cancer cells, lung endothelia and residual immune cells. Recent gene-expression studies that profiled metastases established in mouse models after injection of human cancer cells have shown striking difference between populations of the cells that colonize distinct organs, suggesting that many potential factors, in addition to surface molecules, may determine organ-specific metastasis [34, 35]. Obviously, better understanding of main mechanisms and factors governing lung metastasis development will improve recent curative strategies and increase life quality for many cancer patients. Study of pulmonary metastasis requires well-established experimental models.

6.3 In *Vitro* Approaches to Recapitulate Certain Steps of Metastatic Process

6.3.1 Conventional Cell Culture Methods

Attempts to experimentally model metastasis begin with rudimentary *in vitro* assays designed to recapitulate individual facets of the metastatic process such as cell adhesion, motility and invasion. Adhesive properties of cancer cells can be investigated by treating cells with anti-bodies binding specifically certain adhesion molecules on cancer cell surface. In some setting such *in vitro* experiments may closely reflect an *in vivo* situation [36]. Resistance cells to anoikis is being evaluated by culturing cells on non-adherent surface while colony forming ability can be estimated by plating sell at low density on adherent surface or in soft agar. Results of these assays may be correlated with certain *in vivo* properties of cancer cells [37]. The cell motility, for instance, can be observed by videomicroscopy or measured by so-called "wound-healing" assay. The cellular invasion is often measured using a Boyden chamber (or transwell chamber) which constitutes a barrier in culture through which cellular invasion can be monitored and estimated qualitatively. Basic *in vitro* approaches are described in details in Chapter 3 of this issue and elsewhere in cell culturing manuals. However, it should be considered that these assays do not reflect specificity of lung tissue architecture as well as specific aspects of lung metastasis.

6.3.2 Lung Organotypic 3D Models

The complex three-dimensional architectural structure of lung parenchyma assumes connections of alveolar units to airways and the close proximity of capillary network. Considering specific sponge-like texture of lung tissue, simple co-culturing of alveolar and endothelial cells is not sufficient to mimic it. 3D lung organotypic model can be created by using collagen or gelatin sponge (Gelfoam) that may serve as a scaffold for organotypic cells co-culture and may be used to study initial events of lung metastasis development. The porous structure of the Gelfoam provide with possibility of microscopic imaging and histological analysis of co-culture. This approach was successfully realized in several studies of lung tissue regeneration, angiogenesis and lung metastasis [38, 39], however this method is quite laborious. Co-culturing lung-derived cells and cancer cells assumes their syngenic nature. Xenograft cancer/immuno-deficient host setting is theoretically acceptable as well; however no data are published so far. In their study, Martin and colleagues used lung-derived cell mixture from FVB mice and syngenic cancer cell line R221A previously isolated from a mammary tumor in the fat pad of a MMTV-PyVT transgenic mouse in the FVB/n background [40]. Cancer cells were labeled with green

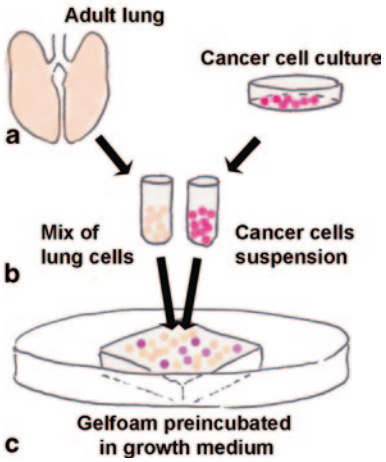

Fig. 6.1 Setup of the 3D lung organotypic co-culture assay. After the lung cells are completely dissociated **a** and most of the red cells are removed, cells suspension is washed and placed on top of the Gelfoam sponge in parallel with suspension of cancer cells **b** in a tissue culture dish containing media. **c** Prolonged incubation allow cells to penetrate inside of Gelfoam and form co-culture mimicking lung tussue.

fluorescent protein (GFP). Protocol of the procedure is adopted from [39] with minor modifications. Setup of the assay is presented in Fig. 6.1**.**

- To construct the cultures, lungs are taken from 6−8 week old mice and completely dissociated overnight at 30°C in digestion solution
- Gelfoam is aseptically cut into 2cm^2 squares and placed into 35 mm culture dishes
- Small needles were placed at two points in the sponge to serve as positional markers for subsequent imaging experiments
- Cancer cells (1.5×10^6) in PBS in a volume of 20 µl are inoculated onto the top of the scaffold
- The digested lung mixture is washed in PBS, while red blood cells are lysed in a solution of PharmLyse (BD Biosciences, San Jose, CA) in PBS.
- The lung cells mixture then is again washed once more in PBS, and 2×10^6 cells in PBS in a volume of 20 µl are also inoculated onto the top of the scaffold.
- The co-cultures is placed at 37°C to allow the cells to soak into the scaffolds.
- One ml appropriate culture media with 15% FCS supplemented with fungizone and antibiotic should then be added to the cultures, and they are placed back into a 37°C incubator
- Culture media is changed daily throughout the experiments
- Before cultures were imaged using confocal microscopy, they are inverted such that the surface of the scaffold where the cells were seeded is flush against the glass surface of the dish.

6.3.3 Ex Vivo Pulmonary Metastasis Assay [41]

Assay was developed quite long ago [42] and modified recently for lung metastasis study [41]. It is still not widely accepted, however it provides with exceptional

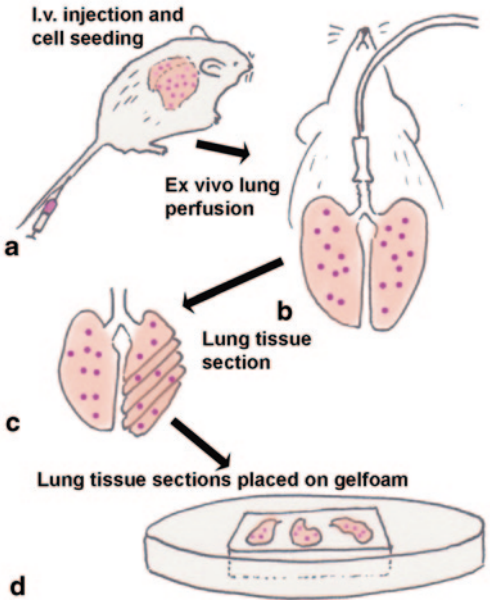

Fig. 6.2 Workflow of ex vivo pulmonary metastasis assay. **a** Fluorescent-labeled tumor cells are delivered to mice by tail-vein injection. **b** Following euthanasia, the trachea is cannulated and attached to a gravity perfusion apparatus. The lungs are infused in the vertical position under a constant 20 cm H2O hydrostatic pressure. The lungs were allowed to cool at 4°C for 20 min to solidify the agarose medium solution. **c** Complete transverse serial sections (1–2 mm in thickness) are gently sliced from each lobe with a scalpel, yielding 16–20 lung slices per pair of lungs. **d** 4–5 lung sections were placed on the sterile Gelfoam sections bathing in culture media

opportunity of real-time assessment of progression from single metastatic cells to multicellular colonies in the lung. The approach allows maintain native lung architecture with all cellular components including migratory cells, type I and type II pneumocytes, alveolar macrophages, vascular endothelial cells, red blood cells, airway-associated epithelial cells, and stromal cells for over three weeks. This assay can be easily applied to study interaction of tumor cells with components of lung tissue as well as for screening of novel anti-metastatic agents at several dose and schedule combinations. As a previous one, this approach assumes utilization clonally related lung tissue and GFP-labeled metastatic cancer cells. Workflow of the assay is schematically shown in Fig. 6.2 while protocol of the procedure is short-cut and adopted from initial publication [41]:

- GFP-positive tumor cells (2×10^5) are delivered by tail-vein injection to mice circulation
- Within 15 min of tumor injection, the mice are euthanized by CO2 inhalation
- Using sterile surgical conditions in a laminar flow hood, the mice are placed in dorsal recumbency. The sternum is removed to expose the lung. The trachea is then cannulated with a 20-gauge intravenous catheter and attached to a gravity perfusion apparatus under constant 20 cm H2O hydrostatic pressure or by syringe infusion of 1.2 ml of well-mixed culture medium/agarose solution at 40°C
- The trachea, lungs, and heart are then carefully removed and immediately placed in a cold solution of PBS containing antibiotics streptomycin at 4°C for 20 min to solidify the agarose/medium solution
- Complete transverse sections (1–2 mm in thickness) are made from each lobe using a n.21 scalpel blade, yielding 16–20 lung sections

- Then 4–5 lung sections are placed on a single 1.5 × 0.7-cm sterile Gelfoam section that had been preincubated for 2 hours in a 6-cm tissue culture dish with culture medium
- Lung sections are incubated at 37°C in humidified conditions of 5 % CO2. Fresh culture medium should be replaced and lung tissue sections are turned over with a sterile iris thumb forceps every other day.

Serum-free conditions on the base of M-199 medium is used for lung culture were described in initial study [42], Mendoza and colleagues proposed some modifications of the media [41] applied for lung perfusion and for farther culturing of lung tissue sections. A critical aspect of the assay is the insufflation of 0.6 % agarose to the lung that is necessary to maintain lung structure. However, technical sophistication of the method is justified by possibility to closely recapitulate *in vivo* condition. Mendoza et al. in their article [41] provides with results of parallel *in vivo* and *ex vivo* assays that confirmed validity of the proposed method.

6.4 In Vivo Models of Lung Metastasis

6.4.1 Spontaneous Metastasis from Orthotopic Xenograft or Syngenic Tumor

The complex nature of metastatic processes and certain endurance of metastases development dictate the need for *in vivo* experimental methods that implement all supportive and regulatory systems in the whole organism setting and for a longer duration to compare to *in vitro*/*ex vivo* experiments. The laboratory mouse traditionally represents the most relevant and useful system for these types of studies. Several approaches to model the metastatic process in mouse are utilized, and there are advantages and disadvantages to each.

Optimal recapitulation of the metastatic process, starting from the initial event of cancer cells detaching from the tumor and entering the bloodstream, may be achieved in models with orthotopically growing primary tumors, either xenografts or syngenic. Example of the xenograft model of the human osteosarcoma developing pulmonary metastases was established by Luu and co-workers [43]. The authors used three osteosarcoma cell lines derived from the same osteosarcoma patient; thus, they had a similar genetic background. The parental cells were transformed with the chemical carcinogen (N-methyl-N'-nitro-N-nitrosoguanidine, MNNG) or with the Ki-RAS oncogen. The derivative cell lines exhibited various *in vitro* characteristics in terms of motility, invasion capacity and anchorage independent growth. When these cells were orthotopically injected into the proximal tibia of athymic mice, it was observed that only Ki-RAS-transformed cells were able to metastasize efficiently from the primary site and develop numerous pulmonary metastases; MNNG –transformed cells produced pulmonary metastases only occasionally, whereas pa-

rental cell lines never developed any lung metastases. Thus, by using these three cancer cell lines, a clinically relevant animal model of lung-metastasizing cancer was established. Such a model can facilitate the investigation of different stages of cancer progression and elucidate the potential role of particular molecular factors in lung metastases development.

However, the using of immunocompromised animals does not allow consideration of the impact of the host immune system in cancer progression and metastases development. This factor is particularly important in cases of pulmonary metastatic disease, where certain components of immune system, such as alveolar macrophages or pulmonary dendritic cells, may play a crucial role. Thus, Miretti and co-authors [44] developed a syngenic model of osteosarcoma metastasizing to the lungs using a cell line derived from a spontaneous osteosarcoma in a Balb/c mouse. In contrast to the study described in the previous paragraph, this study found that increased metastatic potency of the cells *in vivo* does not correlated with an increase of motility, invasion ability or anchorage-independent growth capacity assayed *in vitro*. This observation suggests a role of some endogenous host factors, most likely the immune system, in the process of modeling metastases formation. A shortcoming of the syngenic model is a paucity of endogenously originating metastases in the mouse, compared to those associated with human cancer. In some cases, multiple re-injections of the cells into the mice followed by in vitro passages are utilized to select the most aggressive cancer cell clone and to augment the metastatic potential of the cancer cell population [45]. Increased numbers of cancer cells or repeated injections can be used to improve the reproducibility of the experimental model. Alternative way to increase metastatic potential of injected cancer cells is preliminary whole-body irradiation of mice resulting to suppression of host immune activity; however, such an approach will reduce the competence of the syngeneic model.

6.4.2 Pulmonary Tumor Dissemination from Non-Orthotopic Sides/Tail Vein Injection

In some case orthotopic inoculation of tumor cells is neither possible nor necessary. If the first steps of the metastatic process are of scientific interest, a primary tumor can be grown wherever it is relevant or readily accomplished. For instance, cancer cells can be injected into the location of a typical locally-spreading of tumor, such as the peritoneal cavity for rabdomyosarcomas and ovarian cancers [46]. The simplest way to model distant tumor metastases into the lung is formation of a primary tumor in subcutaneous tissue. All the aforementioned models are considered to closely reflect a real metastatic process; however, they are considerably time-consuming and not always adequately reproducible.

The classic approach to model the later stages of metastatic process is an injection of cancer cells directly into the venous bloodstream followed by evaluation of their ability to colonize the lung. Cancer cells can be either syngenic or xenografts. As it is widely accepted, the syngenic model will reflect tumor-host interactions, while the

xenograft model can be used to study specific characteristics of cancer cells. Some technical aspects must be considered if tumor cells are injected directly into the tail vein for both physiological and ethical reasons. The total number of injected cells usually does not exceed 200–300 thousand, the cells must be well-suspended and not form visible conglomerates, the maximum injected volume should not exceed 150–200 μl, and the injection must be given slowly with the mouse kept in a comfortable position to allow sufficient respiration. This technique is routinely used in many labs for a variety of experimental settings. The conventional protocol is included in this chapter because it closely models metastatic dissemination in the lungs. Some practically important aspects and relevant illustrations can be found in the methodological chapter published by Box and Eccles in their Methods in Molecular Biology series [47]. The following protocol is partially adopted from their publication:

- Place a mouse in the restrainer.
- Disinfect the whole tail using an alcohol-dampened swab.
- Gently mix the tumor cell suspension and load into syringe without needle
- Attach a sterile needle and, expel any air bubbles leaving the intended volume for injection
- Rotate the tail to locate one of the two lateral tail veins.
- With the needle bevel facing upward and on the same plane as the tail vein, slide the needle in 2 mm. A slight pull on the syringe plunger should reveal a flash of blood in the needle
- hub confirming correct entry
- Push the plunger in very slowly and deliver the cell suspension. The vein will change from dark to light as the cell suspension temporarily replaces the blood. Any resistance or blanching will indicate the needle is not in the vein.
- Remove the needle from the vein and with a sterile gauze swab, apply slight pressure to the injection site until bleeding has stopped.
- Remove the mouse from the restrainer and return to its cage. Observe the mouse for 5–10 min to ensure no recurrent bleeding or acute respiratory disfunction. Control the mice condition over one hour to exclude any ill effects.

Repeat using a fresh needle and new cell suspension for each mouse (loading a syringe with sufficient cells for multiple mice can lead to blood clotting in the needle between injections)

6.5 Evaluation of Experimental Lung Metastasis in In Vivo Models

6.5.1 Vital (whole body) Visualization

Growth of metastases in the lung of laboratory mice can be visualized *in vivo* by imaging techniques, like conventional radiography, computed tomography (CT), positron emission tomography (PET), bioluminescence (BLU) or fluorescence (FLU)

imaging. These methods require the using of specific contrasting reagents [48, 49], cancer cells expressing luciferase (Luc) or fluorescent protein (GFP, NIR) [44, 50]. An optimal combination of mentioned techniques can considerably increase sensitivity and allow an accurate detection and 3-dimensional localization pulmonary metastases with several mm of size [51]. All these methods are well established however details of procedures can be slightly variable depending on experimental setting. More precise and even semiquantitative analysis of cancer cells in animal lung can be done by intravital fluorescence video microscopy of the mechanically ventilated lungs after tracheotomy [28]. This approach allows even visualize and analyze the process of tumor cells adhesion on the endothelial wall.

6.5.2 Ex Vivo Approaches of Lung Metastasis Evaluation

Ex vivo lung metastases can be visualized with various resolutions. The rough analysis can be done after infusion of the lung samples with India ink solution followed by destaining with Fakete's solution. The tumor nodules do not absorb India ink, which results in the normal lung tissue staining black while the tumor nodules remain white [44]. Alternative approach is staining with Bouin's fluids that provides a contrast of white lesions against yellow lung tissue [52]. Contrasted metastatic nodules can be easily counted and measured (Fig. 6.3a, b). These methods are well accepted for determining tumor load on the lungs, however supposes relative low accuracy and resolution.

Much more sensitive method of ex-vivo visualization of lung metastasis was described recently [53, 54]. By using tumor cells stably expressing the lacZ gene encoding the bacterial enzyme β-galactosidase, authors supposed possibility of even single detection (Fig. 6.3c). This is a low-cost and not equipment-intensive, however, relatively laborious method. Cancer cells should be stably transfected with the lacZ gene encoding the bacterial enzyme β-galactosidase that metabolizes the chromogenic substrate 5-bromo-4-chloro-3-indolyl-beta-D-galactopyranoside (X-Gal) to an insoluble indigo blue dye. It allows highly sensitive and selective histochemical blue staining of tumor cells in mouse tissue ex vivo down to the single cell level. More precise detection of small metastases in the lung tissue can be performed by light microscopy after routine histological H&E staining (Fig. 6.4a) or IGH for human- or tumor- specific markers (Fig. 6.4b).

6.6 Quantitative Real-Time PCR-Based Assay of Xenograft Lung Metastasis Model

Despite thier wide establishment, methods described in previous paragraphs do not allow a quantitative analysis. PCR-based techniques could represent a valid option for sensitive detection of metastatic human cancer cells in mouse tissues and several authors have applied PCR for specific cell detection. For instance, Nitsche and

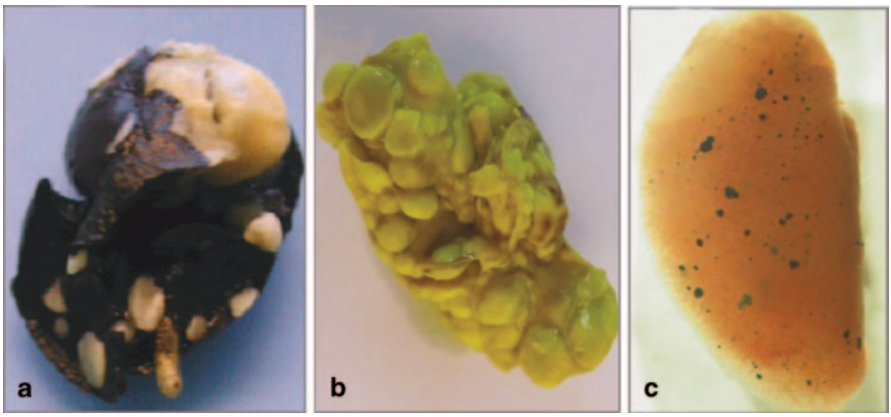

Fig. 6.3 Macroscopic detection of experimental lung metastases. **a** India ink staining (adopted from [44]) **b** Bouin's solutions staining (adopted from [52]) and **c** X-Gal staining for lacZ—expressing cancer cells (adopted from [53])

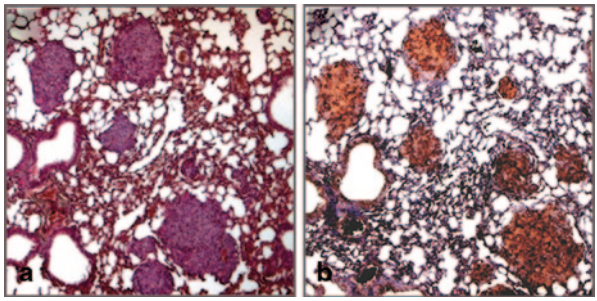

Fig. 6.4 Microscopic detection of experimental lung metastases. Lung metastases developed after i.v. injection of human melanoma cells 1205Lu in nude mice. **a** conventional H&E **b** IHC staining with antibodies against S-100A1 protein

co-authors have described the simultaneous human- and mouse-specific real-time PCR amplification using two different reporter fluorescent dyes to detect xenograft human cells [55]. This method was designed for analysis of blood samples but could be adjusted for any others tissue. However, the threshold of detection was 2 % of human cells, which is barely sufficient in case of solid tumor dissemination. Later, the same group proposed a real-time PCR method based on the amplification of human-specific highly repetitive a-satellite DNA sequences [56]. While the high sensitivity of this technique allowed the detection of one human cell in 10 million mouse cells, it relied on a highly repetitive target sequence in the human genome and thus did not allow reproducible quantification. Likewise, methods based on amplification of the highly repetitive Alu sequence by means of conventional [57] or real-time PCR [58] have the same drawback, since the human genome harbors about 1.1 million copies of the Alu element in a variety of locations and some of them remain actively mobile. This makes it difficult to get equal and reproducible PCR amplification when using primers complementary to the Alu sequence, thus hampering precise quantification. A more accurate detection system was based on an amplification of

Table 6.1 Primers for quantitative real-timePCR assay

(Hu)-specific primers, forward	5′-ctgttttgtggcttgttcag-3′
(Hu)-specific primers, reverse	5′-aggaaaccttccctcctcta-3′
Mouse (Mo)-specific, forward	5′-ttggttgagaagcagaaaca-3′
Mouse (Mo)-specific, reverse	5′-cacacagtcaagttcccaaa-3′

exogenous sequences introduced into the human cell genome prior to the experiment [59]. However, this assay requires a monoclonal population of human cancer cells stably transfected with a specific plasmid, which might interfere with the cell biological properties. Furthermore, the data from this assay must be corrected for the variable number of genomic copies of the plasmid introduced in the cells.

Precise quantification of xenograft metastatic cells in mouse tissue can be done by method described recently [37]. There, species-specific, non-transcribed and conserved regions of the human and mouse genome are selected as targets for PCR amplification. Genomic DNA from the tissue of interest serves as a template for two parallel real-time PCR, and the amount of human cells in a given mouse tissue sample is calculated on the basis of the differences in amplification rates. This method allows highly reproducible detection and quantification of xenograft metastatic cells with the limit of detection below 0.001 % of the total cell number. Method can be applied for almost any type of tissue with consideration of tissue amount taken for analysis. For evaluation of pulmonary metastasis in each experimental animal, it is recommended to use half organ (e.g. right lung) for DNA extraction followed by qPCR analysis and half organ (e.g. left) for routine H&E staining or IHC that allow rough control of the results.

6.6.1 Method Setup

Human (Hu) and mouse (Mo) specific primers for real-time PCR are generated to amplify species-specific, non-transcribed and conserved regions in xenograft (human) and host (mouse) genome. Human (Hu)-specific primers for amplification of 122-bp fragment of a region 7p15-p12 and mouse (Mo)-specific primers for amplification of 181-bp fragment of a region 2F1-F3 of the human and mouse genome, correspondently, are proved and presented in Table 6.1.

These are non-transcribed regions of the human β-actin and mouse β-2-microglobin genes, respectively. One can design other primers pair with consideration of species types (rat, chicken) and optimal length of amplified fragment. Primer specificity must be controlled by conventional PCR before setting of described qPCR-based approach (Fig. 6.5a).

The correlation between the amount of human and mouse DNA in the samples and the amplification efficiency for each primer pair should be estimated to fit the curve and to define equation for experimental data estimation. Any kind of genomic DNA from two species of interest can be utilized for setup the method.

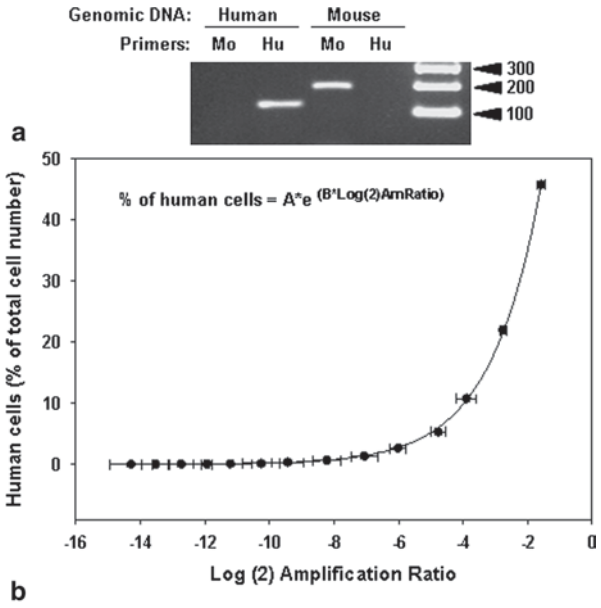

Fig. 6.5 q PCR method setup. **a** Conventional PCR was done with human or mouse genomic DNA and human or mouse -specific primers to confirm the species specificity of both primer pairs. **b** Curve fitting of qPCR data for human and mouse genomic DNA standards. *Y-axis*: Content of human genomic DNA expressed as percentage of human cells (see Table 1 for details). *X-axis*: qPCR quantification shown as mean log(2) Amplification Ratio +/− SD determined in triplicate samples. Adopted from [37]

- A series of standards containing human and mouse genomic DNA with mass percentages of human DNA gradually decreasing from 50 to 0.006 % are prepared (Table 6.2, line 3).
- In order to express the results as percentage of human cells instead of percentage of DNA mass, input data are adjusted for the difference in the size between of the human (~ 3.2 billion bp) and mouse (~ 2.7 billion bp) genomes (Table 6.2, line 4).
- Real-time PCR reactions are performed in parallel with Hu and Mo specific primers with amount of 250–500 ng of DNA mix. Example of resulting Ct are presented in Table 6.2, line 5-6
- The ratios of Hu and Mo amplification rates ('Amp Ratio', Table 6.2, line 7) is calculated as $2^{(CT[Hu]—CT[Mo])}$. The Amplification Ratios underwent $Log_{(2)}$ transformation for easier analysis of samples with low amounts of human DNA (line 8).
- Since standard reactions are performed in three independent experiments, at this stage the average $Log_{(2)}$ Amp Ratio +/− SD for the three paired reactions is calculated (Table 6.2, lines 9–10)
- The results are fitted using a non-linear (logarithmic) regression equation with the amount of human genomic DNA in the sample as the input variable on the x-axis and the $Log_{(2)}$ Amp Ratio on the y-axis (Fig. 6.5b). The value of the independent coefficients A (125.05) and B (0.635) can be determined using SigmaPlot 10.0 software. These coefficients can vary depending on the qPCR kit, equipment, assay conditions and primers, and thus have to be determined for each specific experimental setup.
- To quantify the human cell metastatic load, the initial equation was reversed into a two parameter exponential function ($y=A*exp^{(B*x)}$) where y is the percentage of human cells or human genomic DNA in the sample and x is the Log(2) Amp Ratio.

Table 6.2 Setup of qPCR method

Preparation of standards														
1. Human DNA (ng/μL)	125.00	62.50	31.25	15.63	7.81	3.91	1.95	0.98	0.49	0.24	0.12	0.06	0.03	0.02
2. Mouse DNA (ng/μL)	125.00	187.50	218.75	234.38	242.19	246.09	248.05	249.02	249.51	249.76	249.88	249.94	249.97	249.98
3. Human DNA (% of total)	50.000	25.000	12.500	6.250	3.125	1.563	0.781	0.391	0.195	0.098	0.049	0.024	0.012	0.006
4. Human cells (% of total)	*45.763*	*21.951*	*10.757*	*5.325*	*2.650*	*1.322*	*0.660*	*0.330*	*0.165*	*0.082*	*0.041*	*0.021*	*0.010*	*0.005*
qPCR results and calculations														
5. Ct with human primers	21.780	22.480	23.230	24.040	25.170	26.100	27.190	28.960	29.320	30.470	30.920	31.450	32.770	32.910
6. Ct with mouse primers	20.170	19.650	19.390	19.120	19.200	19.260	19.280	19.460	19.100	19.020	18.920	18.710	18.970	18.920
7. Amplification Ratio	0.328	0.141	0.070	0.033	0.016	0.009	0.004	0.001	0.001	0.000	0.000	0.000	0.000	0.000
8. Log(2) Amp Ratio	−1.610	−2.830	−3.840	−4.920	−5.970	−6.840	−7.910	−9.500	−10.22	−11.45	−12.00	−12.74	−13.80	−13.99
9. Log(2) Amp Ratio mean	−1.577	−2.763	−3.893	−4.770	−6.013	−7.057	−8.220	−9.433	−10.26	−11.21	−11.94	−12.73	−13.52	−14.29
10. Standard deviation (SD)	0.133	0.107	0.304	0.210	0.248	0.419	0.315	0.208	0.173	0.669	0.384	0.230	0.254	0.866
Reverse calculations														
11.Human cells (%)	*46.071*	*21.736*	*10.629*	*6.102*	*2.777*	*1.435*	*0.687*	*0.319*	*0.189*	*0.104*	*0.065*	*0.039*	*0.024*	*0.015*

- Comparison of the experimental data from this reverse calculation with the starting percentage of human cells in the reactions (Table 6.2, line 11 and 4) should show a close correlation, indicating that the method gives correct values over a wide range of human DNA percentage.

6.6.2 DNA Extraction and Real-Time PCR

Any suitable method of genomic DNA isolation and quantitative real-time PCR may be applied. However, considering high sensitivity of PCR it's strongly recommended to stick to the same DNA isolation technique and real-time PCR kit/machine over all steps of the single assay as well as for various experiments are planned to be compared. For the same reason, it is expectable to obtain results variability between experimental animals, therefore using the groups at least for 10 mice is recommended.

- Experimental metastases-bearing mice are harvested, whole lungs are extracted and either froze down with liquid nitrogen or immediately used for DNA isolation.
- Lung tissues is homogenized in urea lysis buffer (2% (w/v) SDS, 10mM EDTA, 0.35M NaCl, 0.1M Tris-HCl, pH 8.0, 7M urea).
- Genomic DNA is extracted (optimally with the standard phenol-chloroform method) and diluted in TE buffer, pH 8.0.
- Real-time PCR is carried out in any suitable LightCycler using the SYBR-Green PCR Master Mix (Applied Biosystems Inc, Foster City, USA) according to the manufacturer's protocol with 250 ng of total genomic DNA. PCR conditions were: 95° for 1 min, 56° for 45 s and 72° for 45 s for 30 cycles, with a first cycle 95° for 10 min.
- In parallel, it is recommended to reproduce several points of standard curve by performing qPCR with several Hu/Mo DNA standard mixtures.

6.6.3 Data Analysis and Statistics

In order to estimate the amounts of human cells in mouse tissues, paired real-time qPCR should be done in triplicate for each sample. Amplification Ratios is determined from the cycle threshold (Ct) according to the formula $R = 2^{(CT[Hu] - CT[Mo])}$ and transformed into $Log_{(2)}R$ for each paired reactions. The percentage of human cells was calculated from the mean values of $Log_{(2)}R$ using the exponential function $Y = A*exp^{(B*X)}$. The A and B constants were determined as described in the section 6.6.1 (see Table 6.2). Results are averaged for each animal.

Averaged results for experimental group of animals are calculated by conventional method. Differences between groups of animals may be assessed with an unpaired two-tailed t-test. Figure 6.6 demonstrate correlation of qPCR (for group of 10 animals) and IHC (one representative example)—based estimation of xeno-

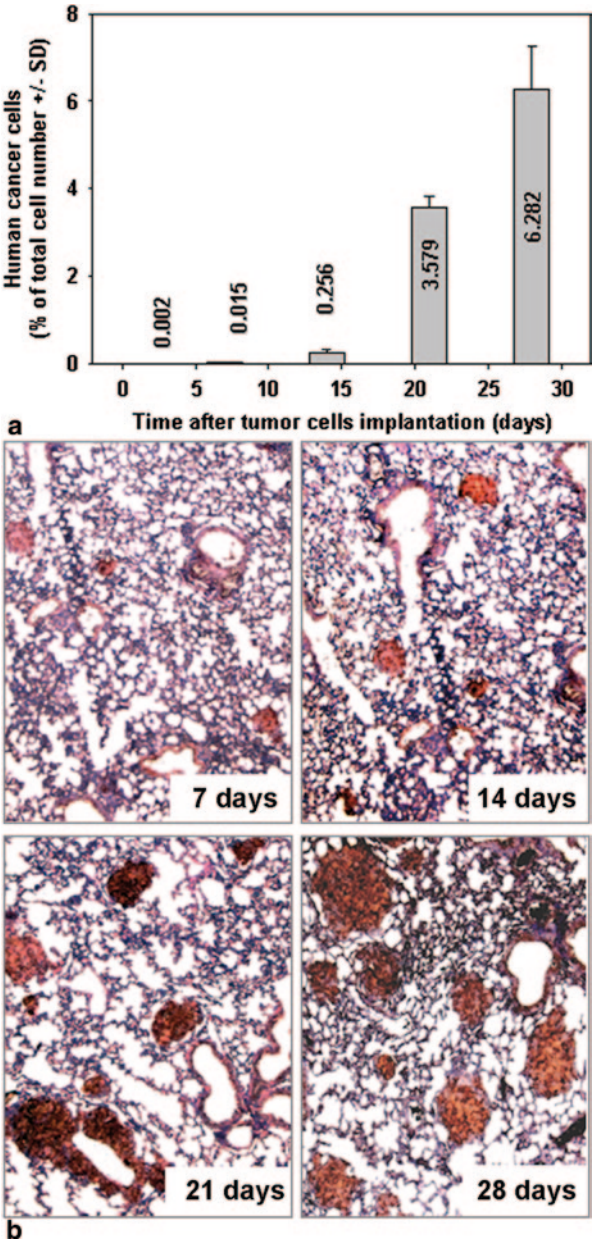

Fig. 6.6 Lung metastases burden estimated by qPCR and IHC. **a** Amounts of metastatic cells in mouse lungs after intravenous injection of human melanoma 1205Lu cells determined by qPCR at 3, 7, 14, 21 and 28 days after cell injection. Results are shown as mean per group ± SD. **b** Tissue sections were prepared from paraffin-embedded specimens of mouse lungs obtained at the same days after cell injection. IHC staining was performed using an anti S-100A1 antibody

graft metastasis burden in lung of nude mice after intravenous injection with human melanoma cells 1205 Lu. Both methods, qPCR and IHC, revealed progressive colonization of lung by tumor cells, however only qPCR approach allow quantification. After being first described in various experimental settings [37], this method was used in others studies by our [60] and others [61] groups.

6.7 Conclusion

As it was mentioned in introduction, metastatic dissemination of lung faces a challenge for practical oncology regardless localization and histological type of primary tumor. Survival rate is currently disappointing, quality of life for patients with advanced secondary cancer of lung is still low while therapeutic approaches are rather palliative.

In parallel with farther investigation of biology of various cancer types that tend to pulmonary colonization, study of proper lung metastasis process is essential and may lead to development of relevant preventive and curative approaches. With considering specific anatomic and physiologic features of the lung that are briefly discussed in this chapter, experimental in *vitro/ ex vivo/ in vivo* models may provide with new insights into general mechanism of pulmonary metastasis. This chapter systematically describes main experimental approaches applied for lung metastasis research with hope to provide researchers with useful theoretical and practical information.

References

1. Ott S, Geiser T (2012) [Epidemiology of lung tumors]. Ther Umsch 69:381–388
2. Schueller G, Herold CJ (2003) Lung metastases. Cancer Imaging 3:126–128
3. Dresler CM, Goldberg M (1996) Surgical management of lung metastases: selection factors and results. Oncology (Williston Park) 10:649–655. (discussion 655–646, 659)
4. Van Schil PE, Hendriks JM, van Putte BP, Stockman BA, Lauwers PR, et al (2008) Isolated lung perfusion and related techniques for the treatment of pulmonary metastases. Eur J Cardiothorac Surg 33:487–496
5. Kycler W, Laski P (2012) Surgical approach to pulmonary metastases from breast cancer. Breast J 18:52–57
6. Vodicka J, Spidlen V, Simanek V, Safranek J, Treska V, et al (2012) [Surgical therapy of pulmonary metastases of colorectal cancer–ten-year results]. Rozhl Chir 91:81–86
7. Osei-Agyemang T, Ploenes T, Passlick B (2012) [Pulmonary metastasectomy: indication and technique]. Zentralbl Chir 137:234–241
8. Schlijper RC, Grutters JP, Houben R, Dingemans AM, Wildberger JE, Raemdonck DV, Cutsem EV, Haustermans K, Lammering G, Lambin P, Ruysscher DD (2013) What to choose as radical local treatment for lung metastases from colo-rectal cancer: Surgery or radiofrequency ablation? Cancer Treat Rev. doi: 10.1016/j.ctrv.2013.05.004
9. Surveillance epidemiology and end results (SEER)—Statistical reports provided by National Cancer Institute (NCI) / U.S. National Institute of Health (NIH) on web site: http://seer.cancer.gov/statistics/
10. Hemminki K, Riihimaki M, Sundquist K, Hemminki A (2013) Site-specific survival rates for cancer of unknown primary according to location of metastases. Int J Cancer 133:182–189
11. Horsfield K (1978) Morphometry of the small pulmonary arteries in man. Circ Res 42:593–597
12. Townsley MI (2012) Structure and composition of pulmonary arteries, capillaries and veins. Compr Physiol 2:675–709
13. Guntheroth WG, Luchtel DL, Kawabori I (1992) Functional implications of the pulmonary microcirculation. an update. Chest 101:1131–1134

14. Guntheroth WG, Luchtel DL, Kawabori I (1982) Pulmonary microcirculation: tubules rather than sheet and post. J Appl Physiol 53:510–515
15. Gehr P, Mwangi DK, Ammann A, Maloiy GM, Taylor CR, et al (1981) Design of the mammalian respiratory system. V. Scaling morphometric pulmonary diffusing capacity to body mass: wild and domestic mammals. Respir Physiol 44:61–86
16. Garcia-Roman J, Zentella-Dehesa A (2013) Vascular permeability changes involved in tumor metastasis. Cancer Lett 335:259–269
17. Claesson-Welsh L, Welsh M (2013) VEGFA and tumour angiogenesis. J Intern Med 273:114–127
18. Criscuoli ML, Nguyen M, Eliceiri BP (2005) Tumor metastasis but not tumor growth is dependent on Src-mediated vascular permeability. Blood 105:1508–1514.
19. Stephen Paget S (1889) The distribution of secondary growths in cancer of the breast. Lancet 133(3421):571–573
20. Mendoza M, Khanna C (2009) Revisiting the seed and soil in cancer metastasis. Int J Biochem Cell Biol 41:1452–1462
21. Auerbach R, Lu WC, Pardon E, Gumkowski F, Kaminska G, et al (1987) Specificity of adhesion between murine tumor cells and capillary endothelium: an in vitro correlate of preferential metastasis in vivo. Cancer Res 47:1492–1496
22. Nicolson GL, Belloni PN, Tressler RJ, Dulski K, Inoue T, et al (1989) Adhesive, invasive, and growth properties of selected metastatic variants of a murine large-cell lymphoma. Invasion Metastasis 9:102–116
23. Okegawa T, Pong RC, Li Y, Hsieh JT (2004) The role of cell adhesion molecule in cancer progression and its application in cancer therapy. Acta Biochim Pol 51:445–457
24. Saiki I (1997) Cell adhesion molecules and cancer metastasis. Jpn J Pharmacol 75:215–242
25. Muller A, Homey B, Soto H, Ge N, Catron D, et al (2001) Involvement of chemokine receptors in breast cancer metastasis. Nature 410:50–56
26. Elzarrad MK, Haroon A, Willecke K, Dobrowolski R, Gillespie MN, et al (2008) Connexin-43 upregulation in micrometastases and tumor vasculature and its role in tumor cell attachment to pulmonary endothelium. BMC Med 6:20
27. Zhu DZ, Cheng CF, Pauli BU (1991) Mediation of lung metastasis of murine melanomas by a lung-specific endothelial cell adhesion molecule. Proc Natl Acad Sci U S A 88:9568–9572
28. Gassmann P, Kang ML, Mees ST, Haier J In vivo tumor cell adhesion in the pulmonary microvasculature is exclusively mediated by tumor cell–endothelial cell interaction. BMC Cancer 10:177
29. Krishnan V, Bane SM, Kawle PD, Naresh KN, Kalraiya RD (2005) Altered melanoma cell surface glycosylation mediates organ specific adhesion and metastasis via lectin receptors on the lung vascular endothelium. Clin Exp Metastasis 22:11–24
30. Ingersoll SB, Langer F, Walker JM, Meyer T, Robson T, et al (2009) Deficiencies in the CD40 and CD154 receptor-ligand system reduce experimental lung metastasis. Clin Exp Metastasis 26:829–837
31. Huh SJ, Liang S, Sharma A, Dong C, Robertson GP (2010) Transiently entrapped circulating tumor cells interact with neutrophils to facilitate lung metastasis development. Cancer Res 70(14):6071–6082
32. Ballas ZK, Buchta CM, Rosean TR, Heusel JW, Shey MR (2013) Role of NK cell subsets in organ-specific murine melanoma metastasis. PLoS One 8:e65599
33. Jordan JL, Nowak A, Lee TD (2010) Activation of innate immunity to reduce lung metastases in breast cancer. Cancer Immunol Immunother 59:789–797
34. Lee H, Lin EC, Liu L, Smith JW (2003) Gene expression profiling of tumor xenografts: In vivo analysis of organ-specific metastasis. Int J Cancer 107:528–534
35. Montel V, Huang TY, Mose E, Pestonjamasp K, Tarin D (2005) Expression profiling of primary tumors and matched lymphatic and lung metastases in a xenogeneic breast cancer model. Am J Pathol 166:1565–1579
36. Tuscano JM, Kato J, Pearson D, Xiong C, Newell L, et al (2012) CD22 antigen is broadly expressed on lung cancer cells and is a target for antibody-based therapy. Cancer Res 72:5556–5565

37. Malek A, Catapano CV, Czubayko F, Aigner A (2010) A sensitive polymerase chain reaction-based method for detection and quantification of metastasis in human xenograft mouse models. Clin Exp Metastasis 27:261–271
38. Andrade CF, Wong AP, Waddell TK, Keshavjee S, Liu M (2007) Cell-based tissue engineering for lung regeneration. Am J Physiol Lung Cell Mol Physiol 292:L510–518
39. Martin MD, Fingleton B, Lynch CC, Wells S, McIntyre JO, et al (2008) Establishment and quantitative imaging of a 3D lung organotypic model of mammary tumor outgrowth. Clin Exp Metastasis 25:877–885
40. Martin MD, Carter KJ, Jean-Philippe SR, Chang M, Mobashery S, et al (2008) Effect of ablation or inhibition of stromal matrix metalloproteinase-9 on lung metastasis in a breast cancer model is dependent on genetic background. Cancer Res 68:6251–6259
41. Mendoza A, Hong SH, Osborne T, Khan MA, Campbell K, et al (2010) Modeling metastasis biology and therapy in real time in the mouse lung. J Clin Invest 120:2979–2988
42. Siminski JT, Kavanagh TJ, Chi E, Raghu G (1992) Long-term maintenance of mature pulmonary parenchyma cultured in serum-free conditions. Am J Physiol 262:L105–110
43. Luu HH, Kang Q, Park JK, Si W, Luo Q, et al (2005) An orthotopic model of human osteosarcoma growth and spontaneous pulmonary metastasis. Clin Exp Metastasis 22:319–329
44. Miretti S, Roato I, Taulli R, Ponzetto C, Cilli M, et al (2008) A mouse model of pulmonary metastasis from spontaneous osteosarcoma monitored in vivo by Luciferase imaging. PLoS One 3:e1828
45. Jia SF, Worth LL, Kleinerman ES (1999) A nude mouse model of human osteosarcoma lung metastases for evaluating new therapeutic strategies. Clin Exp Metastasis 17:501–506
46. Daniel L, Durbec P, Gautherot E, Rouvier E, Rougon G, et al (2001) A nude mice model of human rhabdomyosarcoma lung metastases for evaluating the role of polysialic acids in the metastatic process. Oncogene 20:997–1004
47. Box GM, Eccles SA (2011) Simple experimental and spontaneous metastasis assays in mice. Methods Mol Biol 769:311–329
48. Denoyer D, Greguric I, Roselt P, Neels OC, Aide N, Taylor SR, Katsifis A, Dorow DS, Hicks RJ (2010) High-contrast PET of melanoma using (18)F-MEL050, a selective probe for melanin with predominantly renal clearance. J Nucl Med 51(3):441–447
49. Nimmagadda S, Pullambhatla M, Stone K, Green G, Bhujwalla ZM, Pomper MG (2010) Molecular imaging of CXCR4 receptor expression in human cancer xenografts with [64Cu] AMD3100 positron emission tomography. Cancer Res 70(10):3935–3944
50. Hanyu A, Kojima K, Hatake K, Nomura K, Murayama H, et al (2009) Functional in vivo optical imaging of tumor angiogenesis, growth, and metastasis prevented by administration of anti-human VEGF antibody in xenograft model of human fibrosarcoma HT1080 cells. Cancer Sci 100:2085–2092
51. Deroose CM, De A, Loening AM, Chow PL, Ray P, et al (2007) Multimodality imaging of tumor xenografts and metastases in mice with combined small-animal PET, small-animal CT, and bioluminescence imaging. J Nucl Med 48:295–303
52. Yang F, Huang W, Li Y, Liu S, Jin M, et al (2013) Anti-tumor effects in mice induced by survivin-targeted siRNA delivered through polysaccharide nanoparticles. Biomaterials 34:5689–5699
53. Arlt MJ, Born W, Fuchs B (2012) Improved visualization of lung metastases at single cell resolution in mice by combined in-situ perfusion of lung tissue and X-Gal staining of lacZ-tagged tumor cells. J Vis Exp:e4162
54. Hauser S, Bickel L, Weinspach D, Gerg M, Schafer MK, et al (2011) Full-length L1CAM and not its Delta2Delta27 splice variant promotes metastasis through induction of gelatinase expression. PLoS One 6:e18989
55. Nitsche A, Becker M, Junghahn I, Aumann J, Landt O, et al. (2001) Quantification of human cells in NOD/SCID mice by duplex real-time polymerase-chain reaction. Haematologica 86:693–699.
56. Becker M, Nitsche A, Neumann C, Aumann J, Junghahn I, et al. (2002) Sensitive PCR method for the detection and real-time quantification of human cells in xenotransplantation systems. Br J Cancer 87:1328–1335.

57. Kim J, Yu W, Kovalski K, Ossowski L (1998) Requirement for specific proteases in cancer cell intravasation as revealed by a novel semiquantitative PCR-based assay. Cell 94:353–362.
58. Schneider T, Osl F, Friess T, Stockinger H, Scheuer WV (2002) Quantification of human Alu sequences by real-time PCR–an improved method to measure therapeutic efficacy of anti-metastatic drugs in human xenotransplants. Clin Exp Metastasis 19:571–582.
59. Eckhardt BL, Parker BS, van Laar RK, Restall CM, Natoli AL, et al. (2005) Genomic analysis of a spontaneous model of breast cancer metastasis to bone reveals a role for the extracellular matrix. Mol Cancer Res 3:1–13.
60. Malek A, Nunez LE, Magistri M, Brambilla L, Jovic S, et al. (2012) Modulation of the activity of Sp transcription factors by mithramycin analogues as a new strategy for treatment of metastatic prostate cancer. PLoS One 7:e35130.
61. Milanesi A, Lee JW, Li Z, Da Sacco S, Villani V, et al. (2012) beta-cell regeneration mediated by human bone marrow mesenchymal stem cells. PLoS One 7:e42177.